UCSF
UC San Francisco Previously Published Works

Title

Prolonged production of reactive oxygen species in response to B cell receptor stimulation promotes B cell activation and proliferation.

Permalink

https://escholarship.org/uc/item/9rr1j7rh

Journal

Journal of Immunology, 189(9)

Authors

Wheeler, Matthew
Defranco, Anthony

Publication Date

2012-11-01

DOI

10.4049/jimmunol.1201433

Peer reviewed

eScholarship.org Powered by the California Digital Library
University of California

NIH Public Access
Author Manuscript
J Immunol. Author manuscript; available in PMC 2013 November 01.

Published in final edited form as:
J Immunol. 2012 November 1; 189(9): 4405–4416. doi:10.4049/jimmunol.1201433.

Prolonged production of reactive oxygen species in response to BCR stimulation promotes B cell activation and proliferation

Matthew L. Wheeler[*,†] and **Anthony L. DeFranco**[*]

[*]Department of Microbiology & Immunology, University of California, San Francisco, CA 94143, USA

[†]Graduate Program in Biomedical Sciences, University of California, San Francisco, CA 94143, USA.

Abstract

We have investigated the intracellular sources and physiological function of reactive oxygen species (ROS) produced in primary B cells in response to B cell antigen receptor (BCR) stimulation. BCR stimulation of primary resting murine B cells induced the rapid production of ROS that occurred within minutes, and was maintained for at least 24 h following receptor stimulation. While the early production of ROS (0-2 h) was dependent on the Nox2 isoform of NADPH oxidase, at later stages of B cell activation (6-24 h) ROS were generated by a second pathway, which appeared to be dependent on mitochondrial respiration. B cells from mice deficient in the Nox2 NADPH oxidase complex lacked detectible early production of extracellular and intracellular ROS following BCR stimulation, but had normal proximal BCR signaling and BCR-induced activation and proliferation *in vitro,* and mounted normal or somewhat elevated antibody responses *in vivo.* In contrast, neutralizing both pathways of BCR-derived ROS with the scavenger N-acetylcysteine resulted in impaired *in vitro* BCR-induced activation and proliferation, and attenuated BCR signaling through the phosphatidylinositol 3-kinase pathway at later times. These results indicate that the production of ROS downstream of the BCR is derived from at least two distinct cellular sources and plays a critical role at the later stages of B cell activation by promoting sustained BCR signaling via the PI3K pathway, which is needed for effective B cell responses to antigen.

Introduction

Engagement of the B cell antigen receptor initiates a series of tightly controlled signaling events that in self-reactive B cells promote tolerance, and in B cells responding to foreign antigen promotes activation (1). Signaling downstream of the BCR is initiated by the Src family protein tyrosine kinases Lyn, Fyn, and Blk, which phosphorylate targets to induce activation of a number of signaling pathways required for subsequent B cell responses (2, 3). Among the targets of these kinases are the BCR Ig-α and Ig-β subunits, and their phosphorylation recruits Syk, representing an amplification loop that is countered by several feedback inhibitory pathways (2, 4). An especially well characterized feedback inhibitory pathway involves activation and recruitment, in proximity to the BCR, of the protein tyrosine phosphatase (PTPase) SHP-1, which broadly inhibits signaling by dephosphorylating proximal BCR signaling intermediates such as Syk (5, 6). Feedback inhibition of BCR signaling can also target specific pathways downstream of the BCR, as is the case with the lipid phosphatases PTEN and SHIP, which negatively regulate signaling

Address correspondence and reprint requests to Dr. Anthony L. DeFranco, University of California, 400 Parnassus Avenue, Box 0414, San Francisco, CA 94143. anthony.defranco@ucsf.edu.

$watermark-text
$watermark-text
$watermark-text

$watermark-text

$watermark-text

$watermark-text

through the phosphatidylinositol 3-kinase (PI3K) pathway (7). The balance between the activities of BCR-stimulated protein kinases and the opposing phosphatases is likely critical for controlling the ultimate outcome of antigen encounter by the B cell.

Reactive oxygen species (ROS) have long been known to be potent inhibitors of PTPases and the lipid phosphatase PTEN, through their ability to oxidize catalytic-site cysteines in these enzymes to render them transiently inactive (8-11). While NADPH oxidase-derived ROS production by phagocytic cells is well appreciated for its role in anti-microbial defense, non-phagocytic cells, including lymphocytes, are also known to express functional machinery of the NADPH oxidase complex, and can generate ROS in response to activating signals such as antigen receptor engagement (12-14). Activated cells also generate ROS as a by-product of normal mitochondrial respiration (15). Thus, it has been hypothesized that low-level production of ROS serves as a mechanism to inhibit phosphatase activity and thereby promote BCR signal amplification (16). Interesting in this regard, growth factor receptor signaling, which has many parallels to antigen receptor signaling, has been shown to be amplified by low-level ROS generation (17, 18).

Several studies have investigated whether low-level production of ROS downstream of the BCR or TCR can influence the magnitude of signaling or cell activation in response to cognate antigen stimulation (12, 19-22), however the results have been inconclusive, and were focused mainly on the signaling function of ROS generated early after antigen receptor engagement. In this study, we sought to examine the role of ROS production in regulating BCR signaling both at early times upon initial stimulation, and later during the activation of mature B cells. We found that ROS production in response to BCR stimulation arises from two distinct sources; one that is dependent on the Nox2 isoform of NADPH oxidase and occurs within minutes of BCR crosslinking, and a second that occurs at later times following BCR stimulation and is likely derived from mitochondrial sources. Importantly, we found that B cells deficient in early Nox2-dependent ROS production had no major defects in proximal BCR signaling or B cell activation, and mounted normal or enhanced antibody responses to a T cell-dependent antigen. In contrast, neutralizing ROS produced at later times attenuated BCR-dependent sustained PI3K signaling, and ultimately resulted in defective activation and proliferation in response to BCR stimulation. These results show that while early NADPH oxidase-derived ROS is dispensable for BCR signal amplification in naïve resting B cells, the continuous production of ROS at later times during the activation process is critical for maintaining some components of BCR signal transduction, and for optimal antigen-induced B cell activation and proliferation.

Materials and Methods

Mice

Mice were between the ages of 7-12 weeks for most experiments. B6 (000664; C57BL/6J) and Ncf1 mutant mice (004742; C57BL/6J-*Ncf1m1J*/J) (24) were purchased from Jackson laboratory. MD4 transgenic (Ig^{HEL}) mice were obtained from J. Cyster (University of California, San Francisco) and crossed to the *Ncf1m1J*/J background for some experiments. All animals were housed in a specific pathogen-free facility at the University of California San Francisco, according to University and National Institutes of Health guidelines. Animal use was approved by the University of California Institutional Animal Care and Use Committee.

Antibodies, flow cytometry analysis, and B cell purification

Fluorophore-conjugated Abs directed against the following molecules were used: B220 (RA3-6B2), CD23 (B3B4), CD86 (Gl1), CD69 (H1.2F3), CD95(Fas), GL7 (Ly77), IgD

$watermark-text

$watermark-text

$watermark-text

(11-26c.2a) and CD19 (ID3) all from BD Pharmingen; CD24 (M1/69) from Biolegend; CD93 (AA4.1) from eBioscience; IgM (goat polyclonal F(ab) monomer, μ chain specific) from Jackson immunoresearch. Cells were analyzed on an LSR-II (BD Pharmingen). B cell populations in the spleen and bone marrow were stained for 30 min with anti-B220-PE-Cy7, CD93-APC, CD23-PE, and IgM-FITC F(ab) monomer, and mature and immature B cell subpopulations were distinguished using the Allman protocol (52). Dead cells were excluded by propidium iodide (BioChemika) uptake. Purified B cells were isolated from spleens of 7-12 week old mice by negative selection using CD43 microbeads (Miltenyi Biotech) according to the manufacturer's instructions, and passage through MACS LS separation columns (Miltenyi Biotech). All FACS data were analyzed with FlowJo version 9.3.3 (Tree Star software).

Detection of ROS

Cytochrome-C reduction to measure extracellular ROS production was performed as described (53). Briefly, purified splenic B cells were resuspended in phenol red free HBSS with Ca/Mg salts + 1% BSA at 5×10^6 cells/ml, equilibrated at 37°C for 10 min. Cells (100 μl) were aliquoted into wells of Immulon-4 96 well plates (Thermo Scientific) containing cytochrome C (sigma) (0.1 mM final concentration). Immediately following addition of stimulus (50 μg/ml anti-IgM $F(ab')_2$, 500 μM PMA, or 500 ng/ml HEL for MD4 B cells) OD recordings at 550nm and 490nm were read at 2 min intervals in a 96 well kinetic plate reader (Molecular Devices; Spectra MAX plus). Relative superoxide production was derived from change in OD at 550-490nm.

Chemiluminescent detection of superoxide was performed as described (21) using Diogenes (National Diagnostics). Briefly, purified B cells were stimulated as described above except in the presence of Diogenes, and luminescence was recorded at 5 min intervals on a luminometer (Molecular Devices; Spectra MAX M5).

BCR-localized ROS production was measured as described (19), by flow cytometry, by stimulating cells with 20 μg/ml anti-IgM $F(ab')_2$ conjugated to OxyBURST Green H_2DCFDA, SE (invitrogen) in phenol red free HBSS w/ Ca/Mg salts + 10mM HEPES + 1% FBS. ROS production was recorded at 488nm at 5 min intervals by flow cytometry using an LSR-II and gating $B220^+CD93^-$ splenic B cells or $B220^-$ non-B cells as a control.

Intracellular superoxide was recorded on total spleen cells loaded intracellularly with 5 μM Mitosox-Red (Invitrogen) for 20 min at 37°C, and stained for surface B220 and CD93 as described above. For short term recordings, B cells were stimulated at 37°C with 20 μg/ml anti-IgM $F(ab')_2$, and Mitosox-Red fluorescence was recorded at 561 nm at 5 min intervals over 30 min by flow cytometry using an LSRII, and gating on mature B cells and non-B cells as described above for anti-IgM-DCFDA. For longer time points, purified B cells were pre-stained with anti-B220 and CD93, stimulated with 10 μg/ml anti-IgM $F(ab')_2$ in complete Iscove's medium containing 10% FBS for 2, 6, 12, and 24 h, and loaded with 5 μM Mitosox-Red for 30 min at 37°C prior to harvesting the cells at each time point. Cells were then washed and analyzed by flow cytometry as described to measure Mitosox-Red fluorescence. In some cases, cells were pre-incubated with 5 mM N-acetylcysteine (Sigma) for 30 min prior to stimulation, or treated for the last 2 h of stimulation with 20 μg/ml Antimycin-A (Sigma).

Analysis of calcium mobilization

Measurement of intracellular-free calcium levels was performed as described (54). Briefly, splenocytes were loaded with Indo-1-AM (Molecular Probes, Invitrogen) and stained for B220, CD93 (AA4.1), CD23, and surface-IgM (using F(ab) monomer). Cells were

$watermark-text

$watermark-text

$watermark-text

resuspended in RPMI-1640 medium with 1% BSA and 10 mM HEPES, warmed for 3 min at 37°C, and baseline indo-1 fluorescence was recorded on an LSR-II for 30 s. Cells were then stimulated with 2 or 20 μg/ml goat anti-mouse anti-IgM F(ab')$_2$ (Jackson Immuno Research) and median intracellular calcium levels measured for an additional 3 min, indicated by the ratio of fluorescence 405 nm emission to 530 nm emission over time. For some experiments cells were pre-incubated for 15 min with 5 mM N-acetylcysteine prior to stimulation.

Intracellular Flow cytometry

Intracellular measurement of phospho-ERK, phospho-AKT, and phospho-Syk were performed as described (54). Briefly, 4×10^6 splenocytes were resuspended in Iscove's medium containing 1% BSA, 10 mM HEPES and 2-ME, and pre-warmed at 37°C for 30 min. In some cases, cells were stained for surface IgM (with anti-IgM F(ab) monomer) for the final 10 min of warming. Cells were stimulated with 25 μg/ml anti-IgM F(ab')$_2$ for 2, 10, and 30 min and immediately fixed with 2% Paraformaldehyde and permeabilized with 100% ice-cold methanol (both from Electron Microscopy Services). Cells were labeled with anti-phospho-Syk-Alexa-647 (BD Pharmingen), anti-phospho-ERK1/2 (thr202/Tyr204) rabbit mAB, or anti-phospho-AKT (Ser473) rabbit mAB (both from Cell Signaling Technology), followed by staining for anti-rabbit IgG-APC (Jackson Immunoresearch) (for p-ERK and p-AKT) and B220, CD24 (in place of CD93), and CD23. Cells were analyzed by flow cytometry, and the phosphorylation status of each signaling molecule was analyzed within the mature follicular B cell population ($B220^+$, $CD24^-$. $CD23^+$, $IgM^{int\text{-}lo}$). For analysis of late time points purified splenic B cells were stimulated for 12 h with 10 μg/ml anti-IgM F(ab')$_2$ in complete Iscove's medium containing 10% FBS, followed by intracellular staining and flow cytometry as described above using anti-phospho-ERK1/2 or anti-phospho-S6 (Cell Signaling Technology) rabbit mAB's. In some cases stimulation was carried out in the presence of 5 mM NAC (added prior to stimulation or for the last 2 h of stimulation) or 1 μM of the class I PI3K inhibitor GDC-0941 (Chemdea) added for the last 2 h of stimulation.

B cell activation and proliferation

For *in vitro* B cell activation analysis, purified splenic B cells were resuspended at 1×10^6 cells/ml in complete Iscove's medium containing 10% FBS, in the presence or absence of 5 mM NAC, and equilibrated at 37°C for 30 min prior to stimulation. Following stimulation with anti-IgM F(ab')$_2$, cells were harvested at indicated times, and stained with fluorescent antibodies against surface CD69 (6-7 h) or CD86 (18 h). For *in vitro* proliferation, purified B cells, in the presence or absence of 5 mM NAC, were stimulated as described above with 10 μg/ml anti-IgM F(ab')$_2$, 500 ng/ml CpG (Integrated DNA Technologies), or 10 μg/ml anti-CD40 (BD Pharmingen) + 10 ng/ml IL-4 (Roche). BrdU (BD Pharmingen) was added to cells (final concentration 10 μM) 36 h after stimulation, and cells were harvested for analysis 48 h after stimulation. Proliferation was assessed by incorperation of BrdU within $B220^+$ cells by intracellular staining using a BrdU flow kit (BD Pharmingen) following manufacturers instructions. Cells were analyzed by flow cytometry using an LSR-II, and proliferation was derived from the percentage or absolute number of BrdU positive B cells.

Immunizations, Germinal center cell analysis, ELISA, and ELISPOT

To assess T cell-dependent antibody production, mice were injected intraperitoneally with 50 μg NP-CGG precipitated in Alum. Sera were collected on days 7 and 14 after immunization, and NP-specific IgM and IgG_1 titers were measured by ELISA. For ELISA, 96 well plates (BD Falcon) were coated overnight with NP_{10}-BSA and blocked with 2% FBS in 1×PBS (1-2 h), followed by incubation with serial dilutions of serum for 2 h at room temperature. NP-specific IgM and IgG1 were detected with Horseradish peroxidase (HRP)-

$watermark-text

$watermark-text

$watermark-text

conjugated anti-mouse IgM and IgG1 Abs (Southern Biotech) and developed with TMB substrate (Vector laboratories). OD (450-570 nm) measurements were recorded with a 96 well microplate plate reader (Molecular Devices; VERSA max). Serum antibody titers were derived from the slope of the titration curve and normalized to a standard serum sample from a hyper-immunized mouse. Germinal center cell development was measured on days 7 and 14 from NP-CGG immunized mice by staining total spleen cells with antibodies against B220, CD4, IgD, CD95 (Fas), and GL7, and defining GC B cells as $B220^{+}$, IgD^{-lo}, Fas^{+}, and $GL7^{+}$. Numbers of NP-specific plasma cells were determined by ELISPOT. Briefly, splenocytes from NP-CGG immunized mice were resuspended in complete Iscove's medium containing 10% FBS, and incubated overnight in wells of multiscreen HTS 96 well filter plates (Millipore) that were previously coated with NP_{10}-BSA. The following day, plates were washed of cells and spots were detected with HRP-conjugated anti-mouse IgG (Southern Biotech) and developed with a 3-Amino-9-ethylcarbazole (AEC) chromogen kit (Sigma), according to manufacturer's instructions.

B cell antigen presentation

Splenic cells (2×10^5) from WT and $Ncf1^{-/-}$/ MD4 Ig-transgenic were pulsed with indicated concentrations of HEL-Ova (gift from J. Cyster UCSF) for 2 h, and washed to remove excess antigen. Ag-pulsed B cells were then incubated with 1×10^{5} CFSE-labeled ovalbumin-specific OT-II TCR transgenic CD4+ T cells. After 72 h of co-culture, cells were harvested and stained for CD19 and CD4, and OT-II proliferation was determined by monitoring CFSE dilution by flow cytometry, as described. Dead cells were excluded by propidium iodide uptake.

Results

BCR stimulation of primary mouse B cells induces the rapid production of reactive oxygen species

Non-phagocytic cells are known generate low levels of ROS in response to various stimuli such as growth factors or antigen receptor engagement (23). Using several assays that detect superoxide (O_2^-) and/or hydrogen peroxide (H_2O_2), we observed that BCR stimulation of primary splenic B cells induced a measurable oxidative burst in response to BCR stimulation. For example anti-IgM $F(ab')_2$ stimulation induced the extracellular production of O_2^- which could be observed as early as 6 min and was maintained for at least 1 h following BCR stimulation, as measured by reduction of cytochrome C added to the outside of cells (Fig. 1A). In addition, stimulation of B cells with the diacylglycerol (DAG) analogue PMA resulted in robust superoxide production, suggesting that BCR-induced ROS production by B cells is dependent on a DAG-stimulated signaling pathway downstream of the BCR (Fig. 1A). Similarly, stimulation of MD4 Ig-transgenic B cells, which express a transgenic BCR specific for hen egg lysozyme (HEL), with soluble HEL induced robust production of O_2^-, while non-transgenic B cells stimulated with HEL showed no detectible response (Fig. 1B). Highly reproducible, albeit low level, production of O_2^- in response to anti-IgM was also detected using a chemiluminescent oxidation sensitive probe, in agreement with a previous report (21). The PMA induced O_2^- burst detected by this assay was similar to what was observed by cytochrome C reduction (Fig. 1C). Finally, as a measure of BCR-localized ROS production, we chemically conjugated anti-IgM $F(ab')_2$ antibodies to the H_2O_2 detection probe, H_2-DCFDA, and used this probe to stimulate splenic B cells as was recently reported (19).

This method allows for flow cytometric measurement of local ROS production that is adjacent to the BCR. Superoxide generated extracellularly can be rapidly converted to H_2O_2, which is capable of diffusing across the plasma membrane into the cytoplasm (16) where it

$watermark-text

$watermark-text

$watermark-text

could act on cytoplasmic targets. In addition, this method can be used to demonstrate that ROS production is from B cells and not from contaminating phagocytic cells by co-staining cells for surface markers to exclude non-B cell populations from the analysis. Using this reagent we observed robust production of ROS specifically from mature splenic B cells as early as 5 min after BCR stimulation, whereas non-B cells did not show detectible fluorescence of this probe (Fig. 1D). Thus, ROS were produced in proximity to the BCR in a rapid and sustained fashion in response to BCR crosslinking.

Early BCR-induced ROS production is dependent on B cell expression of the Nox2-containing NADPH oxidase

While phagocytic cells such as neutrophils are known to generate ROS utilizing the classical Nox2 isoform of NADPH oxidase, a number of additional isoforms of this enzyme have been identified and have been shown to have unique functions in a wide variety of tissues (13). Both the Nox2-containing NADPH oxidase as well as a calcium-regulated isoform, Duox1, have been suggested to be important for lymphocyte ROS production (12, 14, 20, 21). To investigate the source of BCR-induced ROS generation in primary murine B cells, we first assessed the expression of all known Nox/Duox catalytic subunit isoforms by semi-quantitative RT-PCR. Expression of each isoform was compared to a positive control tissue to verify specificity of the PCR products. Messenger RNA encoding the Nox2 “phagocyte oxidase” catalytic subunit was readily detected in B cells, whereas expression of other NADPH oxidase isoforms was very low or undetectable (Fig. 2A). The low level amplification of Nox3 was also observed in control RNA samples that were not reverse transcribed, likely resulting from genomic DNA contamination (data not shown). These data are in agreement with results of transcript microarray data from the Immunological Genome Project (http://www.immgen.org).

We next asked whether the Nox2 phagocyte oxidase complex is responsible for BCR-mediated ROS production by using mice that harbor a loss-of-function mutation in *Ncf1,* which encodes the essential $p47^{phox}$ subunit of the Nox2-containing NADPH oxidase complex (24). Whereas $p47^{phox}$ is required for Nox2 activity, it is dispensable for other Nox/Duox isoforms (13). B cells from Ncf1-deficient mice showed no detectible O_2^- production in response to PMA stimulation, and a substantially reduced response to anti-IgM, as measured by cytochrome C reduction (Fig. 2B). In addition, B cells from Ncf1-deficient mice crossed to the MD4 Ig^{HEL} transgene failed to generate O_2^- upon stimulation with soluble HEL, further indicating that activation of Nox2 downstream of BCR stimulation was mainly responsible for acute ROS production by B cells (Fig 2B). These results are in agreement with a previous study (21) and our own independent observations (data not shown), showing that BCR-mediated ROS, detected by a chemiluminescent probe, were absent in mice genetically deficient in Nox2 ($gp91^{phox}$). In addition, Ncf1-deficient B cells completely lacked early (5-20 min) production of BCR-localized ROS, as measured with anti-IgM-DCFDA, as well as intracellular production and/or accumulation of ROS following BCR stimulation as measured with the intracellular ROS detection probe Mitosox-Red (Fig. 2C and 2D). While the latter reagent is generally used to detect mitochondrial ROS, in our hands this probe readily detected the early wave of ROS produced after BCR stimulation, which was highly dependent on the Nox2 NADPH oxidase (Fig. 2D).

Taken together, these results show that BCR stimulation induces rapid local production and intracellular accumulation of ROS that is highly dependent on B cell expression and activation of the Nox2 isoform of NADPH oxidase. Therefore, Ncf1-deficient B cells serve as an appropriate model for investigating the possible role for early B cell ROS production in regulating proximal BCR dependent signaling events.

$watermark-text

$watermark-text

$watermark-text

Ncf1-deficient mice have relatively normal B cell development and maturation

Because mutations that affect BCR signaling may influence B cell development and maturation, we looked at frequencies of mature and immature B cell sub-populations from Ncf1-deficient mice. Ncf1-deficient mice showed nearly normal ratios of pro- and pre-B cells, newly formed B cells, and mature re-circulating B cells in the bone marrow (Fig. 3B). Ncf1-deficiency did however result in a small but significant increase in the frequency of mature B cells, and concomitant decrease in immature B cell populations in the spleen (Fig. 3C). We also looked at the frequencies of splenic B cell sub-populations in MD4-transgenic Ncf1-deficient mice, as subtle alterations in B cell development can sometimes be masked by changes in the repertoire of expressed BCR's. Fixing the BCR led to small changes in peripheral B cell frequencies, namely a small but significant increase in the percentage of immature T1 cells, as well as a decreased combined frequency of splenic marginal zone and B1 B cell populations (Fig. 3D). Although there were small changes in B cell subpopulation frequencies, deficiency in Nox2 NADPH oxidase activity had only modest effects on B cell development and maturation.

Deficiency in Nox2 NADPH oxidase-dependent early ROS production does not alter proximal BCR signaling or downstream B cell activation and proliferation

ROS molecules such as H_2O_2 have the ability to transiently inhibit phosphatase activity in the cytoplasm through oxidation of catalytic-site cysteine residues within these enzymes (11). Therefore it has been proposed that production of ROS downstream of the BCR may function as a positive feedback signal, by preventing phosphatases such as SHP-1 from inhibiting downstream BCR signaling (16). Since early BCR-induced ROS production was dependent on the Nox2 NADPH oxidase, we compared the magnitude of a variety of signaling reactions in B cells from WT and Ncf1-deficient mice. Ncf1-deficient B cells were similar to WT cells in their ability to flux calcium in response to BCR stimulation with anti-IgM (Fig. 4A). Furthermore, at several time points tested after anti-IgM stimulation (2-30 min), WT and Ncf1-deficient B cells had indistinguishable activation of proximal and downstream BCR signaling pathways, as measured by phosphorylation of the proximal tyrosine kinase Syk, as well as downstream signaling intermediates ERK and AKT (Fig. 4B and data not shown). Syk is thought to be a primary substrate for SHP-1 mediated dephosphorylation (5), so normal activation of this kinase in Ncf1-deficient B cells argues against a role for NADPH oxidase-derived ROS in inhibiting SHP-1 activity downstream of the BCR. Ncf1-deficient B cells were also indistinguishable from WT cells in activation-induced upregulation of the early and late activation markers CD69 and CD86 (B7-2) (Fig. 4C), and they also proliferated normally *in vitro* in response to BCR stimulation with anti-IgM, or BCR-independent stimulation with CpG, or CD40 and IL-4 (Fig. 4D). These results show that while the Nox2 NADPH oxidase complex is required for early BCR-induced ROS production, it is dispensable for BCR signal amplification and downstream activation and proliferation.

Deficiency in Nox2 NADPH oxidase-dependent ROS production does not alter T cell-dependent germinal center formation or B cell antigen presentation, but enhances T cell-dependent antibody production

While we did not observe any major differences in BCR signaling or activation of naïve resting B cells *in vitro*, it is possible that subtle, or activation-dependent differences in signaling may become more apparent in an *in vivo* setting such as during an antibody response. Surprisingly, Ncf1-deficient mice immunized with the T cell-dependent antigen NP-CGG, produced somewhat elevated antigen-specific serum IgM and IgG1 titers (Fig. 5A). This difference did not appear to be due to differences in germinal center formation, as Ncf1 deficient mice had comparable numbers of IgD^{lo}, Fas^{+}, $GL7^{+}$ GC phenotype B cells on days 7 and 14 after immunization (Fig. 5B). We also did not observe any differences in the

$watermark-text

$watermark-text

$watermark-text

numbers of NP-specific plasma cells measured by ELISPOT to detect anti-NP-IgG producing antibody secreting cells (ASCs) from spleens of day 14 immunized mice (Fig. 5C).

Previous studies have shown that Nox2 NADPH oxidase-dependent ROS generation is accompanied by ion and proton fluxes that promote antigen processing and presentation in dendritic cells (25-27). We were therefore curious whether Ncf1-deficient B cells had an altered ability to present antigen to cognate T cells. To test this possibility, Ncf1-deficient MD4 Ig-transgenic B cells were pulsed *in vitro* with various concentrations of a HEL-Ova conjugate and co-cultured with ovalbumin-specific OT-II TCR transgenic T cells to test their antigen presentation capability. Proliferation of OT-II T cells was measured by CFSE dilution as a readout of the cognate T cell response to antigen. Based on this assay, the antigen presentation ability of MD4 transgenic B cells was indistinguishable regardless of whether they had functional Nox2 activity or not (Fig. 5D). Thus, the reason that Ncf1-deficient mice generated somewhat higher titers of antigen-specific antibody was not evident.

While we cannot rule out a B cell intrinsic effect on antibody production resulting from deficiency in Ncf1, these differences could be due to an absence of myeloid-derived ROS, which have been suggested to be immunosuppressive in some contexts (28, 29). In any case, these results indicate that early BCR-mediated production of Nox2-derived ROS does not enhance *in vivo* B cell responses to a T cell-dependent antigen.

BCR stimulation for 6 h or more leads to sustained production of ROS independently of Nox2 NADPH oxidase

Although our results, along with results of an independent study (21), indicate that early BCR-induced ROS production derived from the Nox2 NADPH oxidase does not substantially promote BCR signaling or B cell activation, it should be noted that there are other sources of ROS in cells, including the mitochondria which generate ROS as an intermediate during normal cellular respiration (15). While acute ROS production by BCR-stimulated resting B cells was dependent on the Nox2 NADPH oxidase complex, as described above, we found that after 6 h of anti-IgM stimulation, significant levels of intracellular ROS were present in Ncf1-deficient B cells (Fig. 6A). By 24 h of stimulation, the levels of intracellular ROS seen in Ncf1-deficient B cells were nearly identical to those observed in BCR-stimulated WT B cells (Fig. 6B). This late production of ROS was measured in purified splenic B cells using the intracellular superoxide detection reagent Mitosox-Red, which has been reported to preferentially detect mitochondria-derived ROS (30). Pretreatment of cells with the ROS scavenger N-acetylcysteine (NAC) blunted ROS production in wild type B cells during the first 2 h and blocked further ROS production for at least 12 h. ROS production by Ncf1-deficient B cells was decreased compared to wild type B cells, particularly at early times, and was completely blocked by 5 mM NAC (Fig. 6A and B). These data indicate that intracellular ROS detected by Mitosox-red fluorescence was generated by Nox2 as well as by other mechanisms. The Nox2-independent production of ROS at later times was unlikely to be derived from other NADPH oxidase family members as BCR stimulation for 6 or 12 h did not induce expression of any additional Nox/Duox isoforms (Fig 6C). In contrast, we found the production of ROS in BCR-stimulated B cells could be substantially enhanced by transient treatment with antimycin-A, which blocks complex-III of the electron transport chain and leads to accumulation of mitochondria-derived O_2^- (Fig. 6D) (31). This result indicates B cells stimulated via their BCR for 12 h have highly active mitochondrial respiration, which is known be a significant source of intracellular ROS production in a variety of cell types (15). Taken together, these results demonstrate that B cell activation is characterized by a delayed production of ROS that is

produced independently of the Nox2 NADPH oxidase, and is maintained during prolonged BCR stimulation.

Prolonged ROS production is required for optimal activation and proliferation, and to sustain PI3K signaling in response to BCR stimulation

As prolonged BCR signaling resulted in ROS production from a second source, we next asked if neutralizing the ROS generated by both mechanisms at later times would affect downstream B cell activation. Pretreatment of WT and Ncf1-deficient B cells with 5mM NAC was sufficient to substantially attenuate intracellular ROS accumulation in wild type B cells, and completely block it in Ncf1-deficient B cells (Fig. 6A and B). This dose of NAC resulted in significantly reduced BCR-induced activation as measured by upregulation of the early activation marker CD69 (Fig. 7A). Furthermore, this treatment resulted in a nearly complete block in proliferation of WT and Ncf1-deficient B cells stimulated with anti-IgM (Fig. 7B). Interestingly, NAC pretreatment did not impact proliferation in response to BCR-independent stimulation with anti-CD40 plus IL-4, or with CpG ODN (Fig. 7B), indicating that the effect of 5mM NAC on anti-IgM-induced proliferation was likely not due to toxicity, but rather that prolonged ROS production is a specific requirement for optimal responses to antigen receptor stimulation.

Treatment of WT and Ncf1-deficient primary B cells with 5 mM NAC had only minimal effects on proximal BCR signaling at early times, as determined by normal phosphorylations of Syk and Erk kinases in response to BCR crosslinking (Fig. 7D). A small reduction in BCR-induced calcium mobilization in both WT and Ncf1-deficient B cells was observed (Fig 7C), but it was unclear whether this was due to scavenging of ROS or some other effect, and furthermore was unlikely to explain the near complete block in BCR-induced proliferation observed with 5 mM NAC. Higher concentrations of NAC (25 mM) further attenuated calcium signaling in agreement with a previous report (21) (data not shown), however this likely reflects additional effects on B cells beyond simply scavenging ROS. As treatment of Ncf1-deficient B cells with 5 mM NAC clearly depleted all residual ROS produced over the first 6-12h of anti-IgM stimulation (Fig. 6B), but did not substantially impact early BCR signaling, these results further support the conclusion that early production of ROS plays little if any role in amplifying proximal BCR signaling upon initial stimulation of resting B cells.

To address the mechanism by which ROS promoted B cell activation and proliferation, we asked if this sustained ROS generation could be functioning to maintain signaling downstream of the BCR. After 12 h of anti-IgM stimulation, both WT and Ncf1-deficient B cells, pretreated with NAC to neutralize both mitochondrial and Nox2 NADPH oxidase-derived ROS, showed unaffected levels of ERK1/2 phosphorylation indicating intact MAPK signaling (Fig. 7E). However signaling through the PI3K pathway was severely attenuated by neutralizing intracellular ROS, as phosphorylation of the ribosomal protein S6, a downstream readout of PI3K activity, was largely reduced by pre-treatment with NAC (Fig. 7E). Phosphorylation of S6 at these late time points remained dependent on continuous PI3K signaling downstream of the BCR, as this signal was completely blocked by addition of the highly specific class I PI3K inhibitor, GDC-0941 (32), for the last 2 h of stimulation (Fig. 7F). Importantly, phospho-S6 levels could also be similarly reduced by transient treatment with NAC for the final 2 h of stimulation (Fig. 7F). These results show that continuous signaling through the PI3K pathway requires the sustained production of ROS, and that ROS-dependent amplification of this signaling pathway likely promotes efficient B cell activation and proliferation in response to BCR stimulation.

$watermark-text
$watermark-text
$watermark-text

$watermark-text

$watermark-text

$watermark-text

Discussion

In this study, we investigated the intracellular sources and biological function of ROS produced by primary B cells at early and late times following BCR stimulation. We found that the immediate production of ROS in resting B cells was dependent on the Nox2-containing NADPH oxidase complex, as B cells deficient in an essential component of this complex, $p47^{phox}$ (*Ncf1*), were unable to generate detectible amounts ROS over the first several hours of BCR stimulation. However, examination of proximal BCR signaling, B cell activation, and B cell proliferation of BCR-stimulated Ncf1-deficient B cells indicated the lack of a unique role for early Nox2 NADPH oxidase-derived ROS production in these processes. Moreover, Ncf1-deficient mice mounted normal, or even elevated, antibody responses *in vivo*, further demonstrating that early BCR-induced ROS production does not function to enhance the initial response of B cells to antigen stimulation. In contrast, after several hours of BCR stimulation, a second major source of ROS emerged, likely generated as a product of mitochondrial respiration. Blocking accumulation of ROS at these later times with the ROS scavenger N-acetylcysteine resulted in severely attenuated PI3K signaling, and led to marked defects in downstream B cell activation and proliferation following BCR stimulation. Thus, ROS did not substantially enhance proximal BCR signaling early after stimulation of resting B cells, but prolonged production of ROS played a critical role in enhancing BCR-mediated activation, at least in part by promoting sustained BCR-induced PI3K signaling.

Our results demonstrating that BCR-induced early ROS production did not contribute measurably to the magnitude of BCR signaling, are in agreement with a recent report (21) which showed that B cells deficient in the catalytic subunit of Nox2, $gp91^{phox}$, also failed to generate ROS in response to BCR stimulation, and had no significant defects in proximal BCR signaling. Furthermore, while both Ncf1-deficient mice (this study) and $gp91^{phox}$ deficient mice (21) exhibit some alterations in antibody responses, these differences were modest in magnitude, and furthermore were elevated compared to wild-type mice with respect to levels of antigen-specific antibody titers. The reason for the enhanced T cell-dependent antibody response observed in Ncf1-deficient mice is not evident from these studies, however it is possible that lack of Nox2 NADPH oxidase-derived ROS production in other immune cells is responsible for these differences. In particular, ROS produced by myeloid cells such as macrophages is known to have immunosuppressive effects on T cells during inflammation (28), and furthermore, regulatory T cells deficient in Nox2 have been shown to have reduced suppressive capacity (33, 34) which may be relevant to FoxP3+ T follicular regulatory cells that have recently been demonstrated to regulate germinal center responses (35, 36).

In contrast to our results with resting primary B cells, a previous study by Singh *et al* (22) found that BCR stimulation of a B lymphoma cell line led to ROS production via the calcium-regulated NADPH oxidase isoform Duox1, resulting in transient inactivation of the PTPase SHP-1 and subsequent BCR signal amplification. A recent study also found that TCR stimulation of human T cell blasts induced rapid Duox1-dependent ROS production that was critical for early TCR signal amplification (20). We were unable to detect expression of Duox1 mRNA in primary resting B cells, and moreover, we did not detect any ROS production at early times following BCR stimulation of Ncf1-deficient resting B cells, indicating that Duox1 is not a significant contributor to BCR-induced ROS during the early activation of resting mature B cells. It is possible that expression of Duox1 is a feature of activated, germinal center, or memory B cells, or was acquired by the B lymphoma cell line used (A20) as one of the changes that contributed to immortalized growth and survival. Although we did not observe upregulated expression of Duox1 in BCR-activated B cells *in*

$watermark-text

$watermark-text

$watermark-text

vitro it is possible that this may differ in an *in vivo* setting, or in the context of B cell activation by other stimuli such as TLR ligands or helper T cell-derived signals.

Another recent study examining B cells deficient in the proton channel HVCN1 suggested a positive signaling role for BCR-induced ROS production (19). HVCN1-mediated proton fluxes have previously been shown to be required for maintaining NADPH oxidase activity in neutrophils undergoing oxidative burst (37, 38). B cells deficient in HVCN1 showed a significant, albeit partial, reduction in ROS produced downstream of BCR stimulation, presumably due to the function of HVCN1 in transporting protons out of the cytosol to balance ionic movements created in the process of ROS production by NADPH oxidase. Interestingly, deficiency in HVCN1 also resulted in largely attenuated proximal BCR signaling and B cell proliferation *in vitro*, and impaired antibody responses *in vivo*. These defects were attributed to a role for HVCN1 in B cells to maintain early NADPH oxidase-dependent ROS production that was required for transient inhibition of SHP-1 to promote BCR signal amplification. Our data showing that Ncf1-deficient B cells lack nearly all early BCR-induced ROS production, but have no defect in BCR signaling or activation *in vitro* or *in vivo* indicate that the defects observed in HVCN1-deficient B cells probably reflect other mechanisms by which HVCN1 function contributes to proximal BCR signaling. As lack of HVCN1 in B cells resulted in cytosolic acidification and mitochondrial dysfunction, the BCR signaling and antibody response defects seen in HVCN1-deficient B cells could result from effects on a number of biochemical processes. Therefore, while an important role for proton translocation is identified by analysis of HVCN1-deficient B cells, the exact mechanism by which this contributes to BCR signaling remains to be defined.

While Richards *et al* (21) and we found that the early Nox2 NADPH oxidase-dependent ROS production does not play a significant role in amplifying proximal BCR signaling, it is known that B cells require continual BCR stimulation for at least 24 h in order to enter the cell cycle and commit to cell division (39, 40). We found that BCR stimulation of naïve resting B cells resulted in prolonged ROS generation, and by 6 h after anti-IgM stimulation a second source of ROS became significant that was independent of the Nox2 NADPH oxidase. Importantly, blocking accumulation of ROS from both sources during this time period with the anti-oxidant N-acetylcysteine severely impaired anti-IgM-induced activation and proliferation of both WT and Ncf1-deficient B cells. In contrast, this anti-oxidant did not inhibit proliferation induced by the TLR9 ligand CpG ODN, or by anti-CD40 plus IL-4, demonstrating that the importance of ROS was restricted to activation through the BCR.

A potential source of Nox2-independent ROS in BCR-stimulated B cells are the mitochondria, which give rise to ROS in the form O_2^- as an intermediate during the electron transport chain (15). Oxygen radicals are normally neutralized with high efficiency by enzymes in the mitochondria, however a small percentage of this ROS is known to leak out of the mitochondria in the form of H_2O_2, which can diffuse through the mitochondrial membrane to potentially oxidize protein cysteine residues and thereby regulate signaling or other physiological processes in the cytosol. It is likely the ROS observed at these later times was derived from the mitochondria, as B cells were found to express negligible amounts of other NADPH oxidase isoforms both in the resting state, or after BCR-induced activation *in vitro*. Moreover, ROS levels could be further enhanced by treating BCR-stimulated cells with a mitochondrial complex III inhibitor, a treatment that results in a build up of O_2^- generated from the electron transport chain (41), indicating that activated B cells at these times had highly active mitochondrial respiration. Mitochondrial ROS have recently emerged as critical mediators of signaling in a number of contexts including macrophage cytokine production, inflammasome activation, and growth and proliferation of cancer cells (30, 42, 43). Our data indicate that the functions of mitochondrial ROS can likely be extended to signaling pathways important for B cell activation and proliferation.

$watermark-text

$watermark-text

$watermark-text

The mechanism by which prolonged production of ROS enhanced B cell activation and proliferation is not totally evident from our studies, however, one likely contribution is enhanced activation of the PI3K signaling pathway, which is an important regulator of cell energy uptake and utilization (44, 45). This pathway is negatively regulated by the lipid phosphatase PTEN which is known to be inactivated by ROS through oxidation of an active-site cystine (8). We found that after 12 h of BCR stimulation, neutralizing ROS with the anti-oxidant N-acetylcysteine had little effect on sustained signaling through the ERK pathway, but this resulted in a marked reduction in phosphorylation of the ribosomal protein S6, which is consistent with an attenuation of upstream PI3K signaling. Furthermore, neutralization of ROS for just the last 2 h of stimulation in B cells treated for 12 h with anti-IgM also reduced S6 phosphorylation, indicating that the continued presence of ROS was required for maintaining this signaling pathway at these later times. We focused on S6 phosphorylation as a readout of PI3K activity in B cells due to the increased sensitivity of this signaling event compared to phosphorylation of AKT at these later times following BCR stimulation, however it will be important to determine if other events downstream of PI3K activation are also similarly reduced by ROS neutralization. In particular, activated AKT is known to phosphorylate and inactivate the transcription factor FOXO1 which normally drives the transcription of genes that maintain cells in a quiescent state (46, 47), and this is consistent with our observation that neutralization of ROS with N-acetylcysteine prevented BCR-induced entry into the cell cycle.

Signaling through the PI3K pathway is critical for a number of cellular processes in lymphocytes including cell proliferation, survival, protein synthesis, and energy utilization, and therefore maintaining signaling through this pathway is likely essential for B cells to respond efficiently to cognate antigen (7, 44, 45, 48). Tonic low-level activation of this pathway is known to be required for the maturation and survival of naïve B cells (49, 50), however, it has also been demonstrated that long-term maintenance of PI3K signaling is critical for B cell proliferation and survival following BCR stimulation (51). The production of ROS at these later stages of B cell activation may therefore represent a mechanism to promote signal amplification when BCR signaling is suboptimal due to moderate antigen affinity, reduced antigen concentration, and/or a reduced number of BCRs present on the cell surface following receptor internalization in response to initial antigen encounter. These results suggest that the amplification of late BCR signaling by ROS is likely critical for efficient B cell responses to T cell-independent antigens, and/or for maintaining the activation status of antigen-stimulated B cells during the early stages of a T cell-dependent antibody response prior to receiving cognate-T cell help.

Acknowledgments

We would like to thank Jason Cyster (UCSF) for providing the MD4 Ig-transgenic mice and HEL-Ova conjugate.

This work was supported by the National Institutes of Health grant RO1 A120038 (to A.L.D.)

Abbreviations used in this paper

ROS	reactive oxygen species
BCR	B cell receptor
NAC	N-acetylcysteine
HEL	hen egg lysozyme
DAG	diacylglycerol

PTPase	protein tyrosine phosphatase
SHP1	Src homology region 2 domain containing phosphatase-1
PTEN	phosphatase and tensin homologe
P13K	phosphatidylinositol 3-kinase
BM	bone marrow
T1	transitional stage 1
T2	transitional stage 2
T3	transitional stage 3
WT	wild type

References

1. Kurosaki T, Shinohara H, Baba Y. B Cell Signaling and Fate Decision. Annu. Rev. Immunol. 2010; 28:21–55. [PubMed: 19827951]
2. Kurosaki T, Hikida M. Tyrosine kinases and their substrates in B lymphocytes. Immunological reviews. 2009; 228:132–148. [PubMed: 19290925]
3. Saijo K, Schmedt C, Su I, Karasuyama H, Lowell CA, Reth M, Adachi T, Patke A, Santana A, Tarakhovsky A. Essential role of Src-family protein tyrosine kinases in NF-kappaB activation during B cell development. Nature Immunol. 2003; 4:274–279. [PubMed: 12563261]
4. Reth M, Brummer T. Feedback regulation of lymphocyte signalling. Nature reviews. Immunology. 2004; 4:269–277.
5. Maeda A, Scharenberg AM, Tsukada S, Bolen JB, Kinet JP, Kurosaki T. Paired immunoglobulin-like receptor B (PIR-B) inhibits BCR-induced activation of Syk and Btk by SHP-1. Oncogene. 1999; 18:2291–2297. [PubMed: 10327049]
6. Xu Y, Harder KW, Huntington ND, Hibbs ML, Tarlinton DM. Lyn tyrosine kinase: accentuating the positive and the negative. Immunity. 2005; 22:9–18. [PubMed: 15664155]
7. Fruman DA, Bismuth G. Fine tuning the immune response with PI3K. Immunological reviews. 2009; 228:253–272. [PubMed: 19290933]
8. Kwon J, Lee SR, Yang KS, Ahn Y, Kim YJ, Stadtman ER, Rhee SG. Reversible oxidation and inactivation of the tumor suppressor PTEN in cells stimulated with peptide growth factors. Proceedings of the National Academy of Sciences of the United States of America. 2004; 101:16419–16424. [PubMed: 15534200]
9. Meng TC, Fukada T, Tonks NK. Reversible oxidation and inactivation of protein tyrosine phosphatases in vivo. Molecular cell. 2002; 9:387–399. [PubMed: 11864611]
10. Rhee SG, Bae YS, Lee SR, Kwon J. Hydrogen peroxide: a key messenger that modulates protein phosphorylation through cysteine oxidation. Science's STKE : signal transduction knowledge environment 2000. 2000:pe1.
11. Tonks NK. Redox redux: revisiting PTPs and the control of cell signaling. Cell. 2005; 121:667–670. [PubMed: 15935753]
12. Jackson SH, Devadas S, Kwon J, Pinto LA, Williams MS. T cells express a phagocyte-type NADPH oxidase that is activated after T cell receptor stimulation. Nature immunology. 2004; 5:818–827. [PubMed: 15258578]
13. Lambeth JD. NOX enzymes and the biology of reactive oxygen. Nature reviews. Immunology. 2004; 4:181–189.
14. Morel F, Cohen Tanugi Cholley L, Brandolin G, Dianoux AC, Martel C, Champelovier P, Seigneurin JM, Francois P, Bost M, Vignais PV. The O2-generating oxidase of B lymphocytes: Epstein-Barr virus-immortalized B lymphocytes as a tool for the identification of defective components of the oxidase in chronic granulomatous disease. Biochimica et biophysica acta. 1993; 1182:101–109. [PubMed: 8394141]

$watermark-text
$watermark-text
$watermark-text

$watermark-text

$watermark-text

$watermark-text

15. Finkel T. Signal transduction by mitochondrial oxidants. The Journal of biological chemistry. 2012; 287:4434–4440. [PubMed: 21832045]
16. Reth M. Hydrogen peroxide as second messenger in lymphocyte activation. Nature immunology. 2002; 3:1129–1134. [PubMed: 12447370]
17. Bae YS, Kang SW, Seo MS, Baines IC, Tekle E, Chock PB, Rhee SG. Epidermal growth factor (EGF)-induced generation of hydrogen peroxide. Role in EGF receptor-mediated tyrosine phosphorylation. The Journal of biological chemistry. 1997; 272:217–221.
18. Sundaresan M, Yu ZX, Ferrans VJ, Irani K, Finkel T. Requirement for generation of H2O2 for platelet-derived growth factor signal transduction. Science. 1995; 270:296–299. [PubMed: 7569979]
19. Capasso M, Bhamrah MK, Henley T, Boyd RS, Langlais C, Cain K, Dinsdale D, Pulford K, Khan M, Musset B, Cherny VV, Morgan D, Gascoyne RD, Vigorito E, DeCoursey TE, MacLennan IC, Dyer MJ. HVCN1 modulates BCR signal strength via regulation of BCR-dependent generation of reactive oxygen species. Nature immunology. 2010; 11:265–272. [PubMed: 20139987]
20. Kwon J, Shatynski KE, Chen H, Morand S, de Deken X, Miot F, Leto TL, Williams MS. The Nonphagocytic NADPH Oxidase Duox1 Mediates a Positive Feedback Loop During T Cell Receptor Signaling. Sci Signal. 2010:3.
21. Richards SM, Clark EA. BCR-induced superoxide negatively regulates B-cell proliferation and T-cell-independent type 2 Ab responses. European journal of immunology. 2009; 39:3395–3403. [PubMed: 19877015]
22. Singh DK, Kumar D, Siddiqui Z, Basu SK, Kumar V, Rao KV. The strength of receptor signaling is centrally controlled through a cooperative loop between Ca2+ and an oxidant signal. Cell. 2005; 121:281–293. [PubMed: 15851034]
23. Finkel T. Signal transduction by reactive oxygen species. The Journal of cell biology. 2011; 194:7–15. [PubMed: 21746850]
24. Huang CK, Zhan L, Hannigan MO, Ai Y, Leto TL. P47(phox)-deficient NADPH oxidase defect in neutrophils of diabetic mouse strains, C57BL/6J-m db/db and db/+ Journal of leukocyte biology. 2000; 67:210–215. [PubMed: 10670582]
25. Mantegazza AR, Savina A, Vermeulen M, Perez L, Geffner J, Hermine O, Rosenzweig SD, Faure F, Amigorena S. NADPH oxidase controls phagosomal pH and antigen cross-presentation in human dendritic cells. Blood. 2008; 112:4712–4722. [PubMed: 18682599]
26. Savina A, Jancic C, Hugues S, Guermonprez P, Vargas P, Moura IC, Lennon-Dumenil AM, Seabra MC, Raposo G, Amigorena S. NOX2 controls phagosomal pH to regulate antigen processing during crosspresentation by dendritic cells. Cell. 2006; 126:205–218. [PubMed: 16839887]
27. Segal AW. How neutrophils kill microbes. Annual review of immunology. 2005; 23:197–223.
28. Gelderman KA, Hultqvist M, Pizzolla A, Zhao M, Nandakumar KS, Mattsson R, Holmdahl R. Macrophages suppress T cell responses and arthritis development in mice by producing reactive oxygen species. The Journal of clinical investigation. 2007; 117:3020–3028. [PubMed: 17909630]
29. Sareila O, Kelkka T, Pizzolla A, Hultqvist M, Holmdahl R. NOX2 complex-derived ROS as immune regulators. Antioxidants & redox signaling. 2011; 15:2197–2208. [PubMed: 20919938]
30. Zhou R, Yazdi AS, Menu P, Tschopp J. A role for mitochondria in NLRP3 inflammasome activation. Nature. 2011; 469:221–225. [PubMed: 21124315]
31. Brookes PS, Yoon Y, Robotham JL, Anders MW, Sheu SS. Calcium, ATP, and ROS: a mitochondrial love-hate triangle. American journal of physiology. Cell physiology. 2004; 287:C817–833. [PubMed: 15355853]
32. Folkes AJ, Ahmadi K, Alderton WK, Alix S, Baker SJ, Box G, Chuckowree IS, Clarke PA, Depledge P, Eccles SA, Friedman LS, Hayes A, Hancox TC, Kugendradas A, Lensun L, Moore P, Olivero AG, Pang J, Patel S, Pergl-Wilson GH, Raynaud FI, Robson A, Saghir N, Salphati L, Sohal S, Ultsch MH, Valenti M, Wallweber HJ, Wan NC, Wiesmann C, Workman P, Zhyvoloup A, Zvelebil MJ, Shuttleworth SJ. The identification of 2-(1H-indazol-4-yl)-6-(4-methanesulfonyl-piperazin-1-ylmethyl)-4-morpholin-4-yl-t hieno[3,2-d]pyrimidine (GDC-0941) as a potent, selective, orally bioavailable inhibitor of class I PI3 kinase for the treatment of cancer. Journal of medicinal chemistry. 2008; 51:5522–5532. [PubMed: 18754654]

$watermark-text

$watermark-text

$watermark-text

33. Lee K, Won HY, Bae MA, Hong JH, Hwang ES. Spontaneous and aging-dependent development of arthritis in NADPH oxidase 2 deficiency through altered differentiation of CD11b+ and Th/Treg cells. Proceedings of the National Academy of Sciences of the United States of America. 2011; 108:9548–9553. [PubMed: 21593419]
34. Efimova O, Szankasi P, Kelley TW. Ncf1 (p47phox) is essential for direct regulatory T cell mediated suppression of CD4+ effector T cells. PloS one. 2011; 6:e16013. [PubMed: 21253614]
35. Linterman MA, Pierson W, Lee SK, Kallies A, Kawamoto S, Rayner TF, Srivastava M, Divekar DP, Beaton L, Hogan JJ, Fagarasan S, Liston A, Smith KG, Vinuesa CG. Foxp3+ follicular regulatory T cells control the germinal center response. Nature medicine. 2011; 17:975–982.
36. Chung Y, Tanaka S, Chu F, Nurieva RI, Martinez GJ, Rawal S, Wang YH, Lim H, Reynolds JM, Zhou XH, Fan HM, Liu ZM, Neelapu SS, Dong C. Follicular regulatory T cells expressing Foxp3 and Bcl-6 suppress germinal center reactions. Nature medicine. 2011; 17:983–988.
37. Morgan D, Capasso M, Musset B, Cherny VV, Rios E, Dyer MJ, DeCoursey TE. Voltage-gated proton channels maintain pH in human neutrophils during phagocytosis. Proceedings of the National Academy of Sciences of the United States of America. 2009; 106:18022–18027. [PubMed: 19805063]
38. Ramsey IS, Ruchti E, Kaczmarek JS, Clapham DE. Hv1 proton channels are required for high-level NADPH oxidase-dependent superoxide production during the phagocyte respiratory burst. Proceedings of the National Academy of Sciences of the United States of America. 2009; 106:7642–7647. [PubMed: 19372380]
39. Damdinsuren B, Zhang Y, Khalil A, Wood WH 3rd, Becker KG, Shlomchik MJ, Sen R. Single round of antigen receptor signaling programs naive B cells to receive T cell help. Immunity. 2010; 32:355–366. [PubMed: 20226693]
40. DeFranco AL, Raveche ES, Paul WE. Separate control of B lymphocyte early activation and proliferation in response to anti-IgM antibodies. J Immunol. 1985; 135:87–94. [PubMed: 3873499]
41. Turrens JF, Alexandre A, Lehninger AL. Ubisemiquinone is the electron donor for superoxide formation by complex III of heart mitochondria. Archives of biochemistry and biophysics. 1985; 237:408–414. [PubMed: 2983613]
42. Bulua AC, Simon A, Maddipati R, Pelletier M, Park H, Kim KY, Sack MN, Kastner DL, Siegel RM. Mitochondrial reactive oxygen species promote production of proinflammatory cytokines and are elevated in TNFR1-associated periodic syndrome (TRAPS). The Journal of experimental medicine. 2011; 208:519–533. [PubMed: 21282379]
43. Weinberg F, Hamanaka R, Wheaton WW, Weinberg S, Joseph J, Lopez M, Kalyanaraman B, Mutlu GM, Budinger GR, Chandel NS. Mitochondrial metabolism and ROS generation are essential for Kras-mediated tumorigenicity. Proceedings of the National Academy of Sciences of the United States of America. 2010; 107:8788–8793. [PubMed: 20421486]
44. Maciver NJ, Jacobs SR, Wieman HL, Wofford JA, Coloff JL, Rathmell JC. Glucose metabolism in lymphocytes is a regulated process with significant effects on immune cell function and survival. Journal of leukocyte biology. 2008; 84:949–957. [PubMed: 18577716]
45. Jones RG, Thompson CB. Revving the engine: signal transduction fuels T cell activation. Immunity. 2007; 27:173–178. [PubMed: 17723208]
46. Yusuf I, Zhu X, Kharas MG, Chen J, Fruman DA. Optimal B-cell proliferation requires phosphoinositide 3-kinase-dependent inactivation of FOXO transcription factors. Blood. 2004; 104:784–787. [PubMed: 15069012]
47. Chen J, Yusuf I, Andersen HM, Fruman DA. FOXO transcription factors cooperate with delta EF1 to activate growth suppressive genes in B lymphocytes. J Immunol. 2006; 176:2711–2721. [PubMed: 16493026]
48. Wullschleger S, Loewith R, Hall MN. TOR signaling in growth and metabolism. Cell. 2006; 124:471–484. [PubMed: 16469695]
49. Calamito M, Juntilla MM, Thomas M, Northrup DL, Rathmell J, Birnbaum MJ, Koretzky G, Allman D. Akt1 and Akt2 promote peripheral B-cell maturation and survival. Blood. 2010; 115:4043–4050. [PubMed: 20042722]

50. Srinivasan L, Sasaki Y, Calado DP, Zhang B, Paik JH, DePinho RA, Kutok JL, Kearney JF, Otipoby KL, Rajewsky K. PI3 kinase signals BCR-dependent mature B cell survival. Cell. 2009; 139:573–586. [PubMed: 19879843]

51. Donahue AC, Fruman DA. Proliferation and survival of activated B cells requires sustained antigen receptor engagement and phosphoinositide 3-kinase activation. J Immunol. 2003; 170:5851–5860. [PubMed: 12794110]

52. Allman D, Lindsley RC, DeMuth W, Rudd K, Shinton SA, Hardy RR. Resolution of three nonproliferative immature splenic B cell subsets reveals multiple selection points during peripheral B cell maturation. J Immunol. 2001; 167:6834–6840. [PubMed: 11739500]

53. Lowell CA, Fumagalli L, Berton G. Deficiency of Src family kinases p59/61hck and p58c-fgr results in defective adhesion-dependent neutrophil functions. The Journal of cell biology. 1996; 133:895–910. [PubMed: 8666673]

54. Gross AJ, Lyandres JR, Panigrahi AK, Prak ET, DeFranco AL. Developmental acquisition of the Lyn-CD22-SHP-1 inhibitory pathway promotes B cell tolerance. J Immunol. 2009; 182:5382–5392. [PubMed: 19380785]

$watermark-text

$watermark-text

$watermark-text

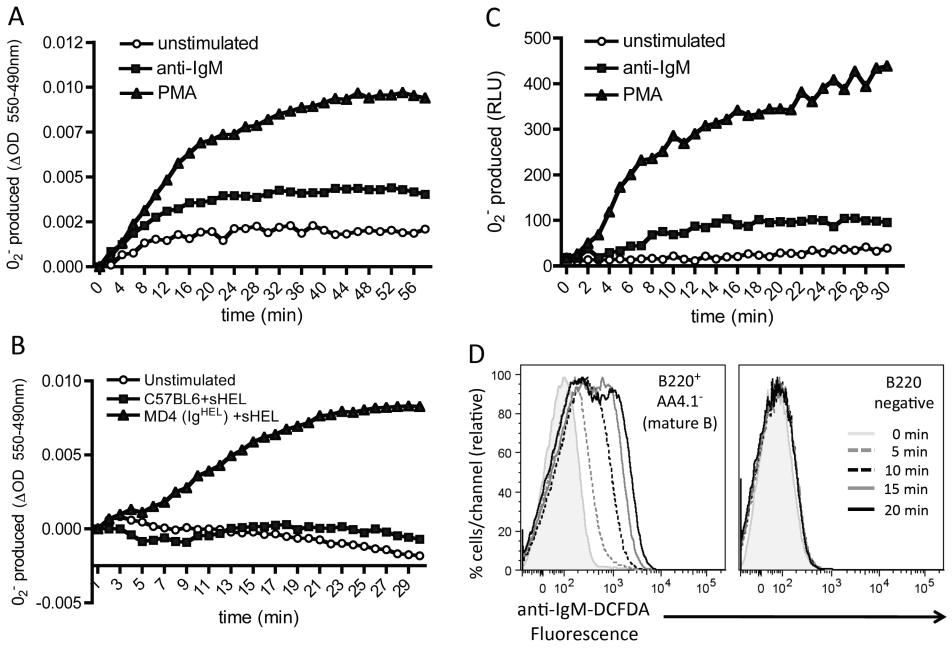

Figure 1. BCR stimulation of primary mouse B cells induces the rapid production of reactive oxygen species

Purified mouse primary B cells (A-C) or total spleen cells (D), isolated from wild-type (A and C) or MD4/Ig^{HEL} (B) spleens, were stimulated for the indicated times with 0.5 μg/ml PMA, 25 μg/ml anti-IgM F(ab')$_2$, 1 μg/ml soluble HEL, or 20 μg/ml anti-IgM-DCFDA. **A)** O_2^- production was measured by cytochrome C reduction from WT B cells which were unstimulated (open circles), or stimulated with PMA (filled triangles) or with anti-IgM (filled squares). Relative O_2^- levels are shown as ΔOD 550nm-490nm at 2 min intervals over 1 h. **B)** O_2^- production by WT non-transgenic (filled squares) and WT/MD4 Ig^{HEL} B cells (filled triangles) stimulated with soluble HEL (solid symbols) or left unstimulated (open circles) was measured by cytochrome C reduction as in A. **C)** O_2^- production by WT B cells was detected using the chemiluminescent reagent Diogenes, and is shown as relative light units (RLU) following stimulation with PMA (triangles) or anti-IgM (squares) **D)** H_2O_2 production in the vicinity of the BCR was measured at the indicated time points by flow cytometry after activation with anti-IgM conjugated to DCFDA. H_2O_2 production was measured as fluorescence in the FITC channel at each time point, and comparing levels in control $B220^-$ (non-B cells) and $B220^+CD93^-$ mature B cells. All data are representative of at least 2-3 independent experiments.

$watermark-text
$watermark-text
$watermark-text

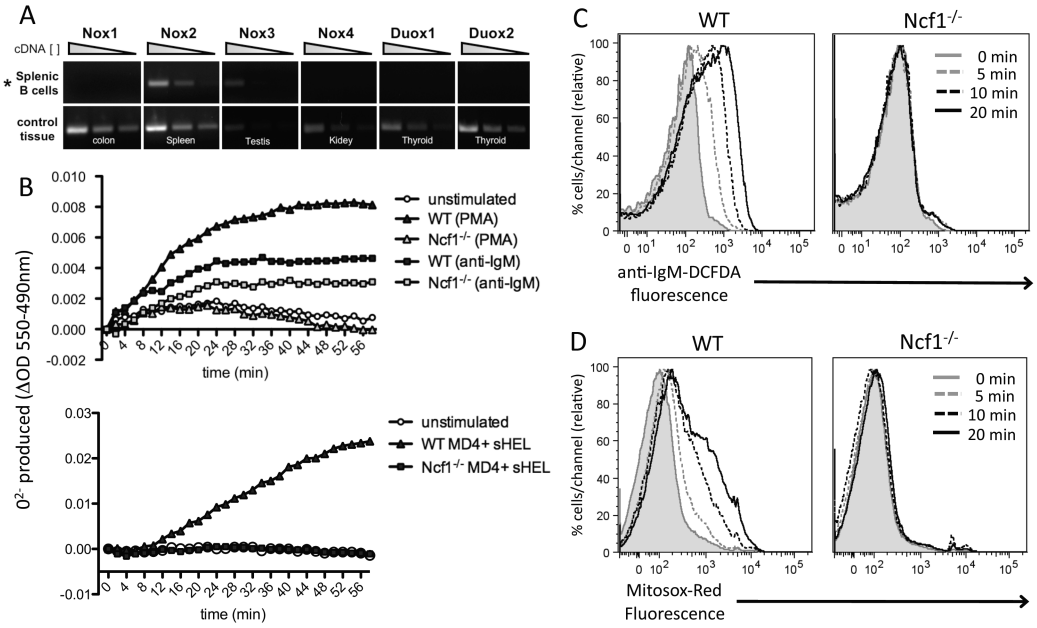

Figure 2. Early BCR-induced ROS production is dependent on B cell expression of the Nox2-containing NADPH oxidase

A.) Expression of NADPH oxidase catalytic subunit isoforms in purified splenic B cells was measured by semi-quantitative RT-PCR using primers specific for Nox1-4 and Duox1-2. Shown are relative amounts of each transcript compared to a positive control tissue for each isoform. Wedges indicate 5-fold serial dilutions of cDNA (starting with 50 ng cDNA). **B.)** (Top panel) O_2^- was measured as in Fig 1A by cytochrome C reduction from B cells isolated from spleens of WT (filled symbols) and Ncf1$^{-/-}$ (open symbols) mice stimulated with PMA (triangles) or anti-IgM (squares) for the indicated times. (Bottom panel) O_2^- was measured by cytochrome C reduction from B cells purified from WT/MD4 (filled triangles) or Ncf1$^{-/-}$/MD4 (filled squares) spleens and stimulated with soluble HEL for the indicated times. Basal ROS levels (open circles; top and bottom panel) were measured from unstimulated WT non-transgenic (top), or WT/MD4 (bottom) B cells. **C)** H_2O_2 production within the vicinity of the BCR was measured by flow cytometry as in Fig 1C from WT and Ncf1$^{-/-}$ B cells stimulated with 20 μg/ml anti-IgM-DCFDA for the indicated times. Shown are relative H_2O_2 levels from mature B cells (B220$^+$CD93$^-$), represented as a histogram for anti-IgM-DCFDA fluorescence. **D)** Intracellular O_2^- production by WT and Ncf1$^{-/-}$ B cells was measured by flow cytometry from cells loaded with the O_2^- indicator dye Mitosox-Red and stimulated for the indicated times with 20 μg/ml anti-IgM. O_2^- production by mature splenic B cells (B220$^+$CD93$^-$) was measured as fluorescence in the PE channel for the indicated time points.

$watermark-text
$watermark-text
$watermark-text

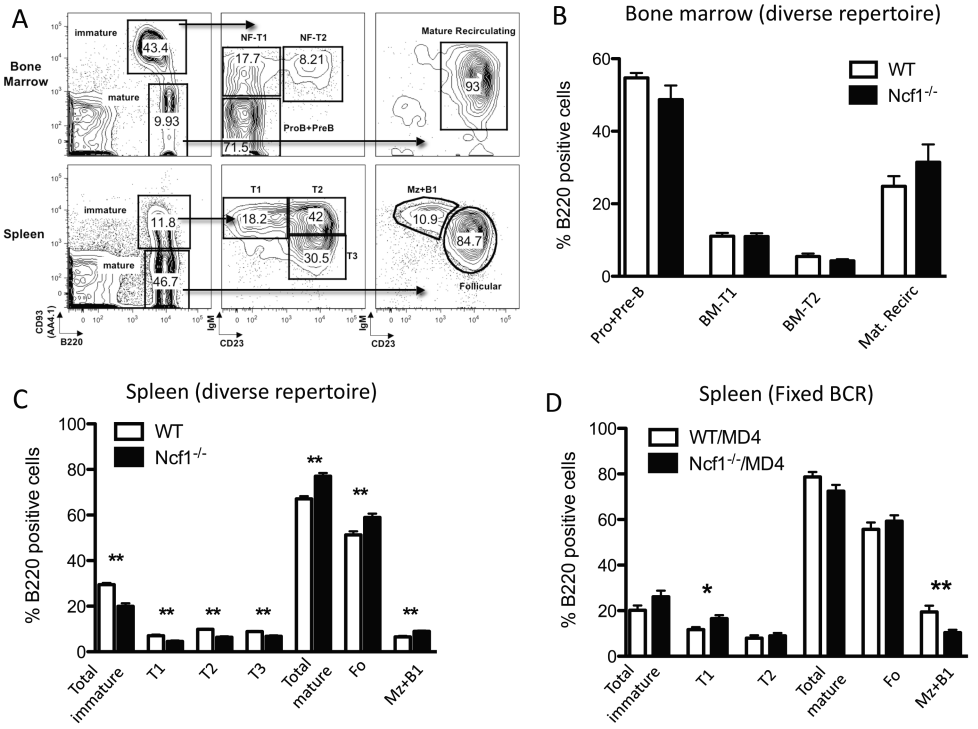

Figure 3. Ncf1-deficient mice have relatively normal B cell development and maturation

A) Representative flow cytometry plots showing gating strategy for bone marrow and spleen B cell sub-populations. Mature and immature B cells in the spleen and BM are distinguished by surface CD93, while follicular, T1, T2, T3, and Mz+B1 (spleen), or mature re-circulating, pro-pre-B, newly formed-T1, and newly formed-T2 (bone marrow) were distinguished by surface CD23 and IgM levels as indicated in representative plots. **B-D)** Frequencies of bone marrow (B) and spleen (C and D) B cell sub-populations are shown as percentages of $B220^+$ cells from WT and $Ncf1^{-/-}$ mice with a diverse (B and C) or fixed (MD4) BCR repertoire (D). Data represent n = 6-12 mice per group and similar results were found in 2-3 independent experiments. (* $p< 0.05$, ** $p< 0.01$ Student's T test)

$watermark-text
$watermark-text
$watermark-text

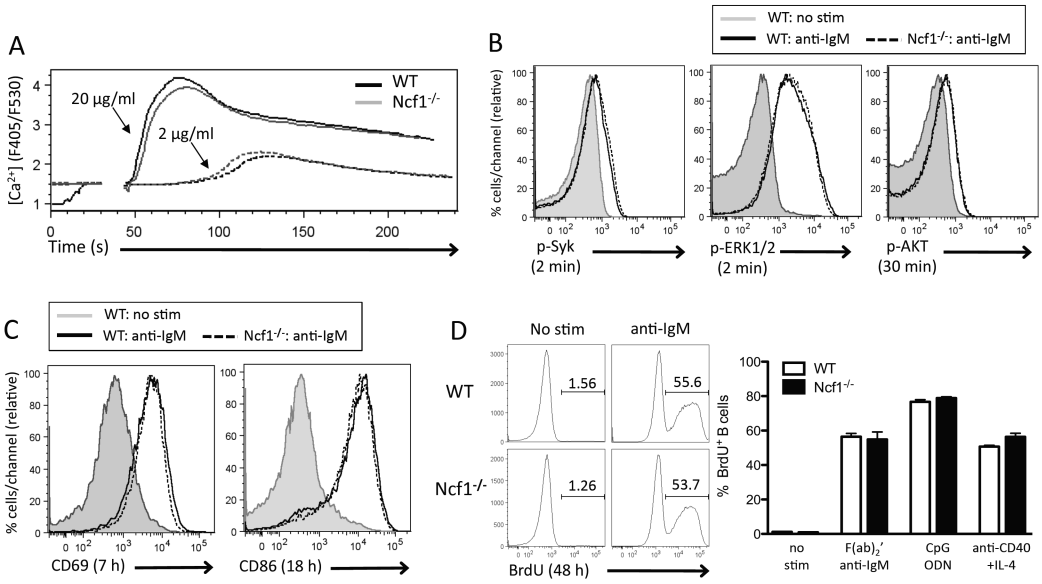

Figure 4. Deficiency in Nox2 NADPH oxidase-dependent early ROS production does not alter proximal BCR signaling or downstream B cell activation and proliferation

A) Cytoplasmic free calcium was measured by indo-1 fluorescence emission ratio at 405 and 530 nm in WT (black lines) and Ncf1$^{-/-}$ (grey lines) follicular B cells (B220^{+}, CD93^{-}, CD23^{+}, IgM$^{int\text{-}lo}$) stimulated with 2 μg/ml (dashed) or 20 μg/ml (solid) anti-IgM. Data are representative of n= 3 mice each from 3 independent experiments. **B)** BCR-induced phosphorylation of proximal (Syk) and downstream (ERK and AKT) targets was measured by flow cytometry in WT (solid black) and Ncf1$^{-/-}$ (dashed black) follicular B cells (B220^{+}, CD24^{-}, CD23^{+}, IgM$^{int\text{-}lo}$) stimulated with 25 μg/ml anti-IgM, and stained intracellulary with phospho-specific antibodies against activating phosphorylation sites of Syk, ERK1/2, and AKT. Basal phosphorylation status is represented by intracellularly stained unstimulated WT B cells (filled grey). Data are representative of n = 2-3 mice each from 3 independent experiments **C)** Upregulation of activation markers CD69 and CD86 was measured by flow cytometry from WT (solid black) and Ncf1$^{-/-}$ (black dashed) purified splenic B cells stimulated for 6 h (CD69) or 18 h (CD86) with 10 μg/ml anti-IgM. Data are representative of n = 2-3 mice in 3 independent experiments. **D)** Proliferation of WT and Ncf1$^{-/-}$ B cells was measured by BrdU incorperation *in vitro* 48 h after stimulation with anti-IgM (10 μg/ml), CpG ODN (500 ng/ml) or anti-CD40 + IL-4 (10 μg/ml and 10 ng/ml). Proliferation was measured by intracellular staining with anti-BrdU and flow cytometry, following an 18 h pulse with BrdU. Left panel shows representative histograms of BrdU^{+} WT (top) and Ncf1$^{-/-}$ (bottom) unstimulated, and anti-IgM stimulated B cells. Data are quantified in right panel as the percentage of WT (white bars) and Ncf1$^{-/-}$ (black bars) that have incorperated BrdU. Data are representative of n = 3 mice/group from 2 independent experiments.

$watermark-text
$watermark-text
$watermark-text

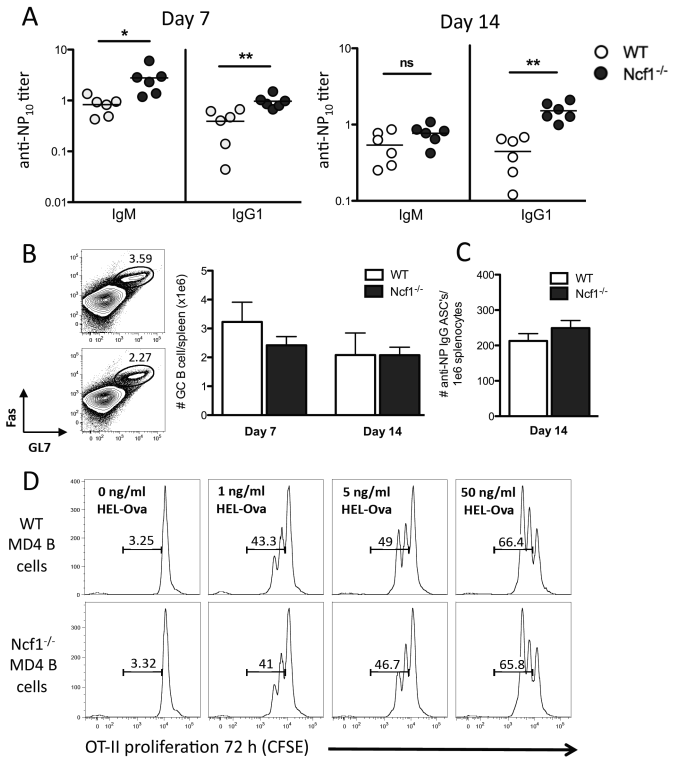

Figure 5. Deficiency in Nox2 NADPH oxidase-dependent ROS production does not alter T cell-dependent germinal center formation or B cell antigen presentation, but enhances T cell-dependent antibody production

A) NP-specific IgM and IgG1 serum antibody titers were measured by ELISA from day 7 and day 14 NP-CGG immunized WT (open circles) and Ncf1$^{-/-}$ (filled circles) mice. Each circle represents an individual mouse (n = 6) (* $p < 0.05$, ** $p < 0.01$). Similar results were found a second independent experiment. **B)** Germinal center formation in response to immunization with T cell-dependent antigen (50 μg NP-CGG in alum IP) in WT and Ncf1$^{-/-}$ mice. Total numbers of GC B cells (IgD^{-low}, GL7^{+}, FAS^{+}) per spleen are shown from day 7 and day 14 NP-CGG immunized WT (white bars) and Ncf1$^{-/-}$ (black bars) mice. **C)** Numbers of anti-NP IgG producing plasma cells per spleen from day 14 NP-CGG immunized WT (white bars) and Ncf1$^{-/-}$ (black bars) mice. **D)** Antigen presentation to cognate T cells by WT and Ncf1$^{-/-}$ B cells was measured by co-culturing CFSE-labeled OT-II T cells with WT/MD4 (top panel) or Ncf1$^{-/-}$/MD4 (bottom panel) B cells pulsed with increasing amounts of HEL-OVA. Presentation of Ova to cognate T cells was determined by measuring OT-II proliferation by CFSE dilution following 72 h of co-culture. Data are representative of n= 3 mice/group from 2 independent experiments.

$watermark-text
$watermark-text
$watermark-text

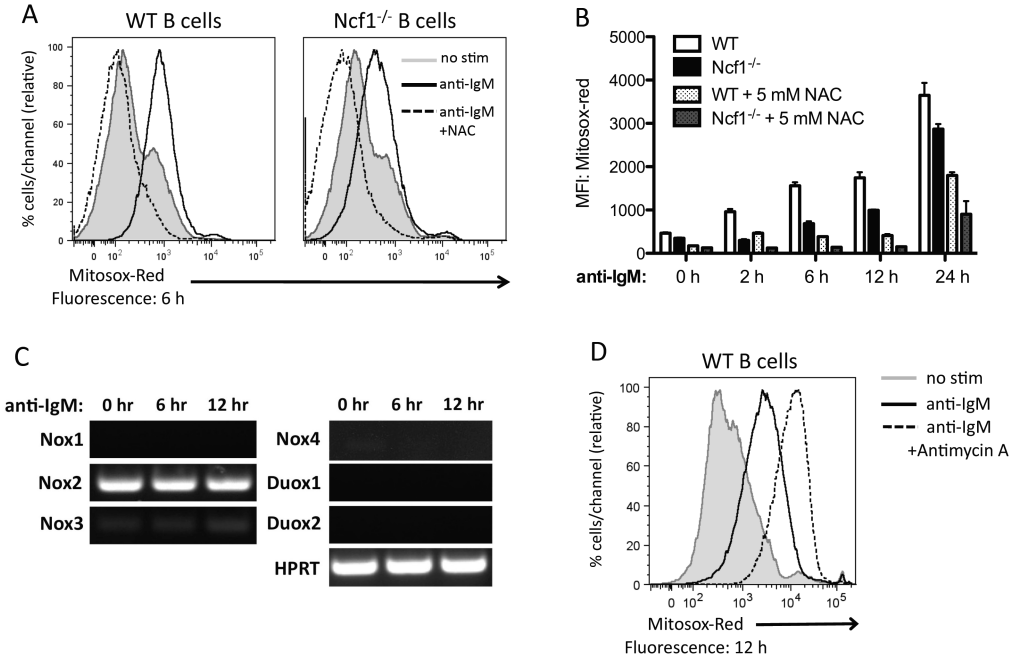

Figure 6. BCR stimulation for 6 h or more leads to sustained production of ROS independently of Nox2 NADPH oxidase

A-B) Purified splenic B cells from WT and Ncf1$^{-/-}$ mice were stimulated with 10 μg/ml anti-IgM for the indicated times, and superoxide levels were measured with the ROS indicator dye Mitosox-Red loaded into cells 30 min prior to harvesting cells at each time point. Specificity of the dye for ROS levels was determined by comparing the median fluorescence intensity (MFI) of Mitosox-Red in WT and Ncf1$^{-/-}$ B cells stimulated in the presence or absence of 5 mM N-acetylcysteine. Histograms (A) represent mitochondrial ROS levels at 0 h (grey filled) and 6 h after anti-IgM stimulation of WT (left) or Ncf1$^{-/-}$ (right) B cells, in the presence (black dashed) or absence (black solid) of 5mM NAC. **B)** Quantification of Mitosox-Red fluorescence (represented as MFI) from WT (white and light grey bars) and Ncf1$^{-/-}$ (black and dark grey bars) B cells measured at the indicated times over 24 h of anti-IgM stimulation in the presence (light grey and dark grey bars) or absence (white and black bars) of NAC. Data are representative of n =3 mice/group from 3 independent experiments. **C)** mRNA Expression of NADPH oxidase isoforms was measured, as described in Fig 2A, from purified resting splenic B cells (0 h), or in purified B cells stimulated for 6 h or 12 h with 10 μg/ml anti-IgM. Data are representative of two independent experiments. **D)** Intracellular superoxide levels were measured as described above with Mitosox-Red from unstimulated (filled grey histogram) and anti-IgM-stimulated WT B cells (12 hrs). Cells were treated for the last 2 h with 20 μg/ml antimycin-A (dashed black) or vehicle control (solid black) to enhance mitochondrial ROS production. Data are representative of n = 2-3 mice/group and similar results were obtained in 2 independent experiments.

$watermark-text
$watermark-text
$watermark-text

$watermark-text
$watermark-text
$watermark-text

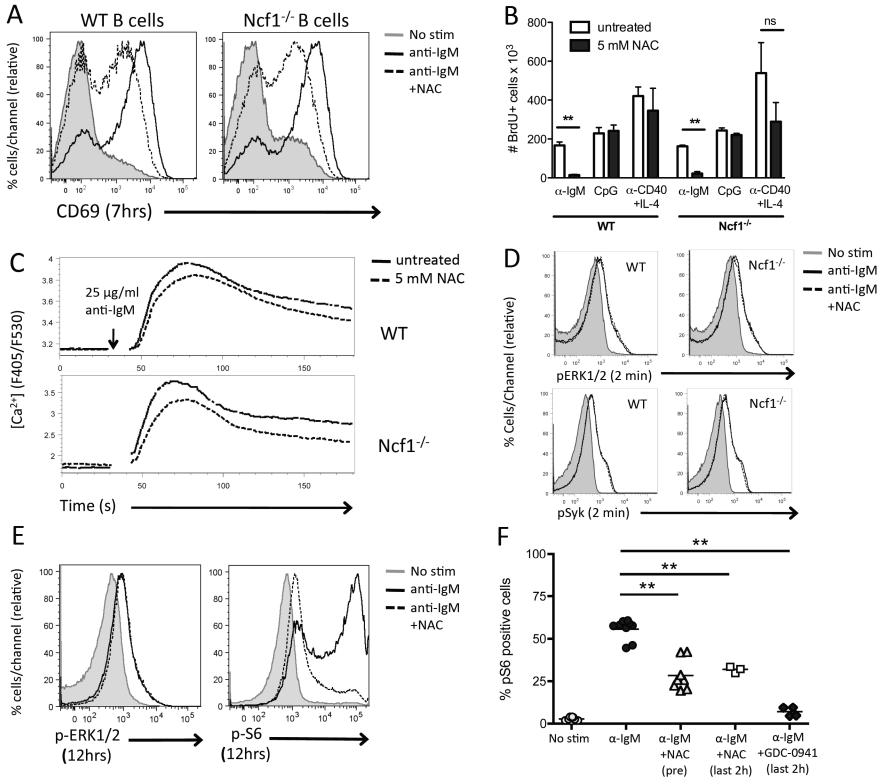

Figure 7. Prolonged ROS production is required for optimal B cell activation and proliferation and for sustained PI3K signaling in response to BCR stimulation

A) Upregulation of the early activation marker CD69 was measured by flow cytometry 7 h after stimulation of WT (left) or Ncf1$^{-/-}$ (right) B cells with 10 μg/ml anti-IgM in the presence (black dashed) or absence (solid black) of 5 mM NAC. Data are representative of n = 2-3 mice/ group. **B)** Proliferation of WT and Ncf1$^{-/-}$ B cells in the presence or absence of NAC was measured by BrdU incorperation as in Fig 3D. Data are represented as the total number of BrdU positive B cells 48 h after stimulation with anti-IgM (10 μg/ml), CpG ODN (500 ng/ml), or anti-CD40 (10 μg/ml) + IL-4 (10 ng/ml) in the presence or absence of 5 mM NAC (** p<0.01). Data from A and B are representative of B cells from n = 2-3 mice/ group, and similar results were found in 3 independent experiments. **C)** BCR-induced calcium mobilization was measured as in Fig 4A in WT (top) and Ncf1-/- (bottom) follicular B cells stimulated with 25 μg/ml anti-IgM in the presence (dashed black lines) or absence (solid black lines) of 5 mM NAC. **D)** BCR-induced phosphorylation of Syk and ERK were measured as in Fig 4B in WT (left panels) and Ncf1-/- (right panels) follicular B cells stimulated with 25 μg/ml anti-IgM in the presence (dashed black) or absence (solid black) of 5 mM NAC. Data are representative of 4 (C) and 3 (D) independent experiments **E)** Phospho-ERK and phospho-S6 levels were measured by intracellular staining and flow cytometry, as described in figure 4b, of purified WT B cells stimulated for 12 h with anti-IgM (10 μg/ml) in the presence (dashed black) or absence (solid black) of 5mM NAC. **F)** Quantification of phospho-S6 (represented as the percentage of p-S6^{+} cells) from purified WT B cells stimulated with anti-IgM, as in E, in the presence or absence of NAC for the entire stimulation (12 h), or incubated for the last 2 h with NAC or 1 μM of the class I PI3K inhibitor GDC-0941. Data represent n=2-3 mice/group, and are pooled from 2-4 independent experiments. (** p<0.01 Student's T test)